nnical Memorandum ERL ARL-75

AN ATTEMPT TO MEASURE ATMOSPHERIC OZONE WITH ULTRAVIOLET LIDAR

Ronald W. Fegley
C. Murray Penney

Air Resources Laboratories
Silver Spring, Maryland
December 1978

noaa NATIONAL OCEANIC AND ATMOSPHERIC ADMINISTRATION / Environmental Research Laboratories

NOAA Technical Memorandum ERL ARL-75

AN ATTEMPT TO MEASURE ATMOSPHERIC OZONE WITH ULTRAVIOLET LIDAR

Ronald W. Fegley
C. Murray Penney

Geophysical Monitoring for Climatic Change

Air Resources Laboratories
Silver Spring, Maryland
December 1978

UNITED STATES
DEPARTMENT OF COMMERCE
Juanita M. Kreps, Secretary

NATIONAL OCEANIC AND
ATMOSPHERIC ADMINISTRATION
Richard A. Frank, Administrator

Environmental Research
Laboratories
Wilmot N. Hess, Director

CONTENTS

NOTICE

Mention of a commercial company or product does not constitute an endorsement by NOAA Environmental Research Laboratories. Use for publicity or advertising purposes of information from this publication concerning proprietary products or the tests of such products is not authorized.

AN ATTEMPT TO MEASURE ATMOSPHERIC OZONE WITH ULTRAVIOLET LIDAR

Ronald W. Fegley and C. Murray Penney

ABSTRACT. NOAA and General Electric attempted to measure the profile of atmospheric ozone with an ultraviolet lidar system in 1975 at the NOAA Mauna Loa Observatory. Differential absorption lidar (DIAL) was used to study the concentration of the species of interest in a wavelength region of strong absorption (in this case 300 nm for ozone). The return signal was inverted to provide the "excess absorption" as a function of height. The excess absorption can then be interpreted as a concentration profile of ozone. The experimental setup, typical data, and an error analysis are discussed. Because of laser difficulties, data quality was not adequate to permit calculation of ozone profiles. Improved capability of commercial lasers makes it likely that excellent results could be obtained with a practical system from 30 km down through the troposphere.

1. INTRODUCTION

A major international monitoring program currently underway is concerned with atmospheric ozone. Because ozone largely determines the quantity and quality of ultraviolet (UV) radiation at the earth's surface, and because it is the primary energy source in and above the stratosphere, it is of great scientific interest (Climatic Impact Assessment Program, 1975). Indeed, because of the great influence ozone has on the global climate, an ambitious monitoring program was reaffirmed at the 1974 Stockholm Conference (Global Atmospheric Research Program, 1975).

The most extensive set of measurements of atmospheric ozone consists of Dobson observations of total ozone made for many years at various geographic locations. Vertical profiles of ozone concentration have been made using balloons and rockets with fair accuracy. Vertical profiles for ozone in the upper stratosphere for the sunlit side of the earth are now available on a continuing basis by means of a BUV sensor aboard the Nimbus IV satellite. Surface ozone concentrations are being monitored at various locations around the world as well.

The NOAA Geophysical Monitoring for Climatic Change (GMCC) program has operated a small network of Dobson instruments for several years and more recently has commenced observations of surface ozone (Geophysical Monitoring for Climatic Change, 1977). During the 1960's a limited number of ozonesonde observations were also made (Hering and Borden, 1965).

One of the recommendations made at the Stockholm Conference was to upgrade the regional ozonesonde networks. At about that time Penney (1974, 1975) presented the possibility of using lidar to make ozone vertical profile measurements. It appeared that lidar might eventually be a superior and less expensive method. Penney's calculations showed that differential absorption lidar (DIAL) in the ultraviolet appeared to be a sensitive lidar method for long-range measurements of atmospheric ozone.

In November 1975, NOAA and the General Electric (GE) Corporate Research and Development Laboratories supported a preliminary UV lidar experiment at the NOAA Mauna Loa Observatory (19.5° N, 155.5° W) near Hilo, Hawaii, to test the feasibility of stratospheric ozone measurements. Several months earlier, a preliminary attempt had been made by Gibson and Thomas (1975). Neither attempt provided data of sufficient quality to produce accurate ozone measurement, primarily because of the limitations of the lasers available at that time. However, the experiments did lay part of the groundwork leading to recent successful results by Megie et al. (1977). In this report we describe our experiment and point out the excellent capabilities for ozone measurements that this approach provides with currently available instruments.

2. THEORY OF THE DIAL TECHNIQUE

In practice, DIAL utilizes the light backscattered from atmospheric molecules and particles in an absorption region for the substance of interest such that absorption by other atmospheric materials is minor by comparison. A reference signal can be obtained when necessary by tuning to a point outside but near the absorption region. The "excess absorption" is then calculated as a function of range from the lidar return signals. This absorption can be directly interpreted in terms of a profile of concentration of the species of interest.

When the strength of the scattering source (molecules and particles) is known to sufficient accuracy (typically ± 1% to 2%), scattering data for a reference wavelength are not needed, and the DIAL measurements can be performed with a single wavelength. This advantage is likely to be realized for stratospheric ozone measurements using UV wavelengths because scattering from particles (the major uncertainty) is less important than molecular scattering in the UV, and because the stratospheric particle loading is usually light. In fact, in lidar

experiments with wavelengths as short as 0.347 μm, it has been very difficult to detect particle contributions to stratospheric scattering (McCormick, 1977). Therefore, initially, we will describe the DIAL technique using a single wavelength. In cases where particles contribute a significant, unknown portion of the scattering, or more than one unknown absorber is present in the measured region, two or more wavelengths must be used. This necessity adds somewhat to experimental complexity and also increases the measurement time moderately (because the laser power must be shared between several wavelengths), but neither disadvantage is critical, and analysis is similar to the one we offer here.

An analysis of the DIAL method at a single wavelength can be explained in terms of the schematic diagram shown in Fig. 1. The outgoing laser beam path is broken up into range elements of length

$$z = \theta c/2 \qquad (1)$$

where z is the length of the range element, θ is the time increment during which light backscattered from z will enter the receiver, and c is the velocity of light.

The range to the jth element is therefore $Z_j = jz$. (2)

The number of detected backscattered photons from the element z_j is given by the lidar equation

$$S_j = \frac{QzA\varepsilon n}{q} (r_j + m_j) T_j/Z_j^2 \quad , \qquad (3)$$

where Q is the energy of the transmitted pulse,

q is the energy per photon (6.6×10^{-19} joules for a wavelength of 300 nm),

A is the effective area of the receiver aperture,

ε is the optical transmission of the receiver,

n is the quantum efficiency of the photomultiplier tube,

T_j is the two-way optical transmission to the jth element,

and r_j and m_j are the Rayleigh and Mie backscatter coefficients, respectively, averaged over the jth range element.

If we take the ratio of the photons received from two range elements, j and k, we find

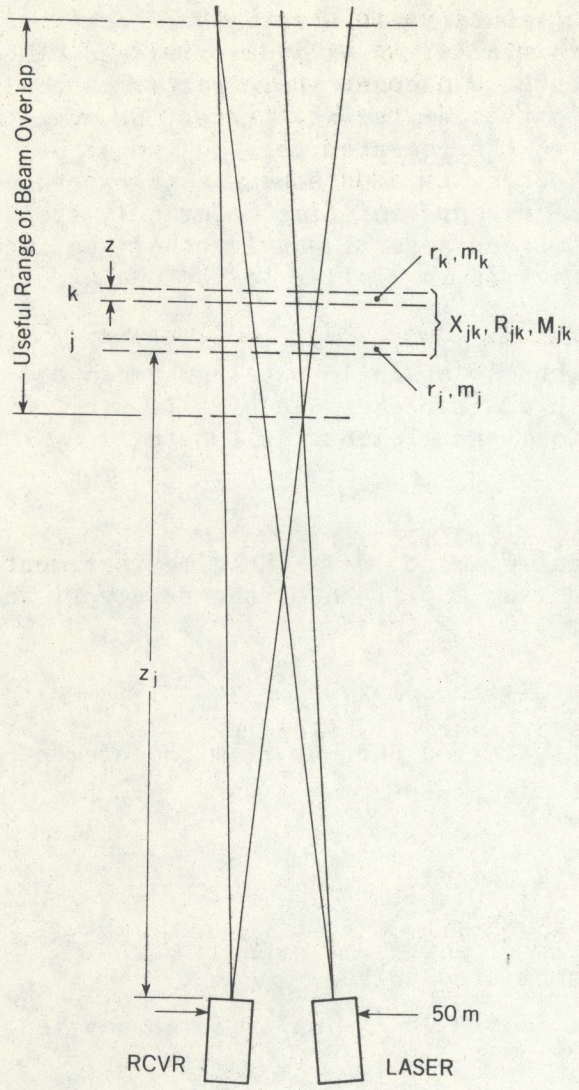

Figure 1. Experimental lidar configuration used at Mauna Loa.

$$N_{jk} \equiv \frac{S_j}{S_k} = \frac{r_j + m_j}{r_k + m_k} \frac{Z_k^2}{Z_j^2} \frac{T_j}{T_k} \quad . \tag{4}$$

The two-way transmission from j to k is given by

$$T_{jk} = \exp\left[-2(k-j)z(R_{jk} + M_{jk} + X_{jk}\,\sigma_x)\right] \tag{5}$$

where R_{jk} and M_{jk} are the Rayleigh and Mie extinction coefficients, respectively, averaged over the interval jk,

X_{jk} is the molecular concentration of the species to be measured, averaged over jk,

and σ_x is the extinction cross section of the species to be measured.

Now,

$$\ln(T_j/T_k) = 2z(R_{jk} + M_{jk} + X_{jk}\,\sigma_x)(k-j) \tag{6}$$

and, solving for the unknown species density, we find

$$X_{jk} = \frac{1}{2\sigma\, z(k-j)} \ln(T_j/T_k) - \frac{1}{\sigma}\,(R_{jk} + M_{jk}). \tag{7}$$

From Eq. (4)

$$\ln N_{jk} = \ln\left(\frac{r_j + m_j}{r_k + m_k}\right) + 2\,\ln(Z_k/Z_j) + \ln(T_j/T_k)\ . \tag{8}$$

Combining (7) and (8), we obtain

$$X_{jk} = \frac{1}{2\sigma_x(k-j)z}\left[\ln N_{jk} - \ln\left(\frac{r_j + m_j}{r_k + m_k}\right) - 2\,\ln(Z_k/Z_j)\right] \tag{9}$$

$$- \frac{1}{\sigma_x}\,(R_{jk} + M_{jk})\ .$$

Equation (9) is the fundamental equation used to obtain concentration of the observed species from DIAL data. The species concentration X_{jk} is determined from the ratio of returns from levels j and k (and any intervening levels). Absorption by any species at lower levels does not change the measured value (although it may deteriorate measurement accuracy by reducing the return signal from levels j and k).

Application of Eq. (9) and the error sources implicit in it will be discussed subsequently. Anticipating this discussion, we note that it is desirable for the observed species to produce 5% to 20% absorption over each range element. The spectral region yielding this absorption for stratospheric ozone levels lies between 280 and 310 nm, where the

ozone Hartley band is characterized by the smooth continuous structure shown in Fig. 2 (Air Force Geophysical Research Office, 1960). It is evident from the figure that the ozone absorption decreases by about a factor of two for each 5 nm increase in wavelength in that range. This behavior allows convenient choice of optimum absorption strength for the region to be probed, without requiring ultra-precise wavelength control.

Laser pulses between 280 and 310 nm can be generated conveniently by doubling the output of a dye laser operating near 600 nm. This approach has the advantage that light at the fundamental wavelength is available in the same beam as the doubled output. Characteristically, 10% to 20% of the light is doubled, and most of the rest propagates through the doubling crystal. Both wavelengths can be transmitted, and the undoubled output can be used as a visible beam for initial alignment to measure particle scatterings and to evaluate the possibility of a significant Mie scattering contribution at the UV wavelength.

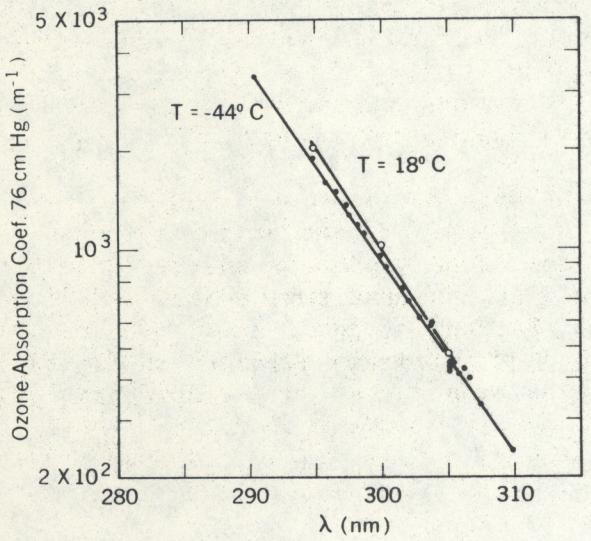

Figure 2. Ozone absorption coefficients versus wavelength at 18 and -44 degrees C. Values are for pure ozone at 76 cm Hg. (Air Force Geophysical Research Office, 1960).

3. NUMERICAL EXAMPLE

To give the reader a better feeling for the magnitudes of the parameters in a typical experiment, a numerical example is presented. We assume a realistic system operating at Mauna Loa Observatory at an altitude of 3.4 km msl. The input parameters are as follows:

Q = 10 J total transmitted energy. This would correspond, for example, to 100 shots at 100 mJ energy each. Currently available pulsed dye lasers (see subsequent discussion) can provide average powers of 10 mW to 200 mW at the doubled wavelength. Thus, 50 to 1000 seconds are required to accumulate the energy assumed here.

$q = hc/\lambda = 6.6 \times 10^{-19}$ J per photon at 300 nm wavelength.

A = 1 m2, the receiver area.

ε = 0.3, the optical efficiency.

n = 0.2, the detector quantum efficiency.

T_j = 0.07, the two-way transmission to the range element at 20 km msl.

Z_j = 16.6 km, the range.

z_j = 1 km, the length of the range element.

$r_j + m_j = 10^{-7} m^{-1}$, the combined Rayleigh and Mie backscatter coefficients at 20 km.

Substituting these values into Eq. (3) yields $S_j = 2 \times 10^3$ photons detected from the element at 20 km. A DIAL measurement concentration of the observed species could be determined from the photon count ratio S_k/S_{k-1}. When each of these total counts is on the order of 2×10^4, the minimum uncertainty in the ratio due to photon counting statistical fluctuation is about ± 1%. Suppose we assume that the ozone absorption from range element k-1 to element k is 20%. Then we can measure this 20% change to a best accuracy of ± 1%, yielding an ozone measurement accuracy of approximately ± 1%/20% or ± 5%. In the next section this estimate will be refined and extended, and other sources of error examined.

4. ERROR ANALYSIS

Rewriting Eq. (9), we will examine it term by term for potential contributions to measurement error:

$$X_{jk} = \frac{1}{2(k-j)\sigma_x z}\left[\ln N_{jk} - \ln\left(\frac{r_j + m_j}{r_k + m_k}\right) - 2\ln(Z_k/Z_j) - 2(k-j)z(R_{jk} + M_{jk})\right].$$

The multiplying term outside the square brackets is known to the extent that the absorption cross section is known. In the case of the ozone Hartley band, the cross section and its weak temperature dependence have been measured by numerous observers, and there is agreement within ± 5%. In fact, agreement is better at these wavelengths than at the slightly longer ones used for Dobson measurement.

Within the square brackets, the first term represents the ratio of photon counts for the two range elements j and k. Errors in this term arise from the statistical fluctuation in photon counts, from background light, and from instrument errors. The first two of these error sources will be examined in some detail subsequently. The importance of instrumental and other errors can be considered qualitatively by noting that the terms within brackets represent approximately the net two-way absorption over the resolution length (k-j)z due to the unknown species. We have noted previously the desirability that this absorption be relatively large, say 10%. Uncertainties in the bracketed factors introduce errors in direct relationship to this net absorption. Thus a residual instrumental error in ln N_{jk} of 0.5%, which should be easily achieved after calibration, will introduce a measurement error of 0.5%/10% or 5%.

The second term in brackets represents the strength of the scattering source. The Rayleigh scattering terms r_j and r_k are products of molecular density times a known cross section; thus they are known to the extent that the altitude distribution of temperature is known. An uncertainty in temperature of 1% from level j to level k will contribute an error of approximately 1%/10% or 10% in the unknown determination.

We have noted previously that the Mie scattering contributions m_j and m_k are normally insignificant for scattering of UV light from the stratosphere, i.e., they are less than 1% of the Rayleigh contributions. In such cases the error contributed by variations in Mie scattering will be necessarily small.

The third term within the square brackets accounts for the $1/Z^2$ signal variation. Since range is determined precisely as a function of time from the lidar return this term will not contribute to errors in the concentration measurement.

The last term within the brackets represents Rayleigh and Mie scattering extinction. These are much smaller than the ozone absorption under typical conditions and, since the small correction they introduce can be calculated with good accuracy, the remnant error introduced by uncertainties in this contribution should be negligible.

We conclude from these qualitative arguments that considerable information can be derived from single UV wavelength DIAL measurements of atmospheric ozone. In particular, such measurements should reveal characteristics of the flow patterns near the tropopause, from observation of variations in the ozone density there. On the other hand, precise quantitative measurements may well require the use of several wavelengths to check possible errors from temperature variations, particle layers, or an interfering unknown absorber in the observed altitude range, such as SO_2.

Daylight background will introduce an additional source of error if it is significant compared with the observed signal, because of the additional statistical fluctuation it adds to the signal. Somewhat shorter wavelengths than 295 nm are advantageous for daytime operation, because of the very rapid falloff of daylight background with wavelength, due to ozone absorption.

The remaining source of error is the variation in signals collected over a given time due to the statistical nature of light scattering and detection. For example, in a series of identical measurements of light energy, for which the average number of detected photons per measurement is $\bar{S}$, the individual measurements will show a standard deviation of $\sqrt{\bar{S}}$.

The calculation of standard deviation for a DIAL measurement is slightly more complicated, because this measurement involves a ratio of counts $N_{jk} = S_j/S_k$. The standard deviation ΔX_{jk} produced by statistical fluctuations in the photon counts can be calculated from the general expression

$$\Delta X_{jk} = \left[\left(\frac{dX_{jk}}{dS_j} \Delta S_j \right)^2 + \left(\frac{dX_{jk}}{dS_k} \Delta S_k \right)^2 \right]^{\frac{1}{2}} . \qquad (10)$$

From Eqs. (4), (9), and (10), we find that the standard deviation for an ozone measurement due to statistical fluctuations in the detected photon counts is given by

$$\Delta X_{jk} = \frac{1}{2\sigma_x (k-j) z} \left(\frac{1}{S_j} + \frac{1}{S_k} \right)^{\frac{1}{2}} . \qquad (11)$$

Figure 3 shows measurement errors predicted by Eq. (11) for experimental parameters corresponding to several different measurement conditions. It is clear that useful results are obtained in the lower stratosphere with practical system parameters. For example, if we transmit 10 J total energy at 305 nm and use a receiver with an area of 1 m^2 and 40% optical efficiency (telescope and filter transmission) we can attain better than 10% accuracy at 25 km and below.

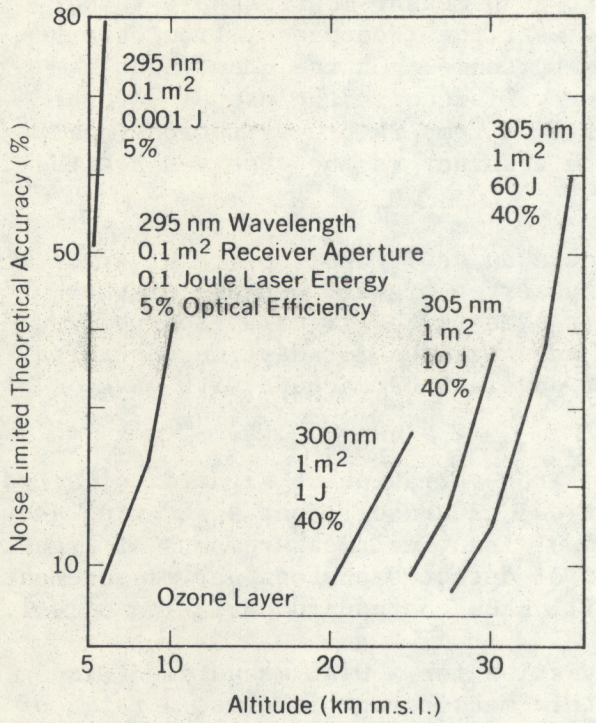

Figure 3. Noise-limited theoretical accuracy as a function of altitude for a lidar at Mauna Loa with different combinations of system parameters. Calculations assume typical ozone profile with peak at 21 km.

5. EXPERIMENTAL SETUP

The experimental configuration is shown in Fig. 1. The transmitter was a Phase-R Corp. model DL-2100 B dye laser that has a maximum output energy of 3 joules per pulse at a wavelength of 590 nm and uses Rhodamine 6-G dye. The optical cavity employed with this laser is shown in Fig. 4. The output of the laser was passed through an ADA crystal doubler where a nominal 295 nm output pulse was produced. Beam energy was monitored, using light reflected from the front surface of the collimating lens. The light passed through a glass UV filter and was diffusely reflected onto a vacuum photodiode detector. The detector output was recorded on a Tektronix storage oscilloscope.

The receiver consisted of a 40-cm-diameter Schmidt Cassegrain telescope with the corrector plate removed in order to achieve higher UV transmission. The collected light passed through a glass UV filter and

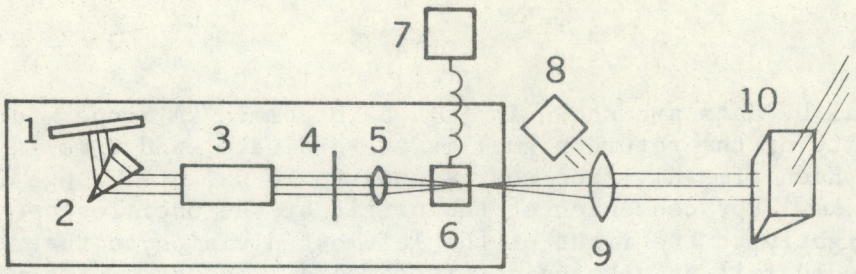

Figure 4. Laser transmitter details: 1. Maximum reflectance mirror. 2. Frequency selecting prism. 3. Flashlamp-dye cell laser head. 4. Partial reflecting mirror. 5. Quartz focusing lens. 6. ADA crystal frequency doubler. 7. Doubler cell temperature controller. 8. Laser pulse energy monitor. 9. Collimating lens. 10. Steering prism/right-angle quartz prism on micrometer mount.

was detected with an EMI 9635Q photomultiplier tube (PMT). The resulting signal was digitized and stored by a Biomation model 8100 transient digitizer. A NOVA minicomputer was used to average and process the return signals. Polaroid photographs of individual returns were made to document the results. Because of the need to use existing components, the receiving system was not optimized for UV work. The telescope mirrors were overcoated with silicon monoxide and therefore had a maximum reflectance of less than 50% at each surface. This reduced the transmission of the telescope to less than 25% of the incoming light. The transmitter and receiver were separated by a distance of 50 m. The receiver was part of an existing lidar system that was already in operation. Because of the rather large separation, the near range of operation was 12 km msl when the system optical overlap extended to 25 km msl.

Optical alignment of the system was accomplished in the following manner: the finder scope of the telescope was used to point the receiver at a known star. Then the laser beam was steered so that it pointed at the same star. It was then usually possible to see the laser beam in the telescope finder scope and make final adjustments so that the laser beam was centered in the finder scope.

A coaxial line ran from the transmitter to the receiver to trigger the data acquisition system when the laser was fired. The data system typically acquired data for 200 μs after being triggered.

The ADA doubler was temperature-tuned to the desired UV output frequency and then the laser frequency was tuned to maximize output energy by adjusting the angle of the maximum reflector. After passing through the doubler, the beam was recollimated with a quartz lens and directed out of the building through a window. The beam was directed upward by a right-angle quartz prism on a micrometer mount.

6. DATA

Typical UV data are shown in Fig. 5 in common "A Scope" format. The intensity of the return signal is the ordinate, and time is the abscissa. Each time division corresponds to 20 μs, or a range increment of about 3 km. For convenience, the origin of the oscilloscope trace was set slightly to the right of the leftmost division so that the major divisons would fall at 3-km height increments. The origin corresponds to 3.4 km (the altitude of Mauna Loa Observatory).

The return signal rises to a maximum at about 9 km msl, then decreases. This maximum is where the fields of view of the transmitter and receiver first overlap completely (see Fig. 1).

The signal consists mostly of spikes representing individual detected photons, except in the region around 9 km, where the spikes begin to blend into a continuous signal. Each of these spikes corresponds to the detection of a single photon. The reader is referred again to Fig. 5 to see that, at the longer ranges, the photon arrival rate is indeed quite low for 1 mJ of transmitted energy. For example, at 20 km the arrival rate is less than 1 photon per 6.7 μs interval. In this case it is necessary to integrate many shots to get good statistics.

The calibrated laser-shot energy monitor was recorded for each shot, and we measured maximum UV energies of 5 mJ. One mJ was more common, but zero UV output was by far the most common occurrence. This variation in pulse energy and the low average pulse energy represent a performance level far below that expected. The reasons for this shortfall will be discussed in Section 7.

Figure 6 demonstrates the essential absence of background photons from the skylight. At the right side of the photo, after all laser photons have returned, there is a completely quiet background. This

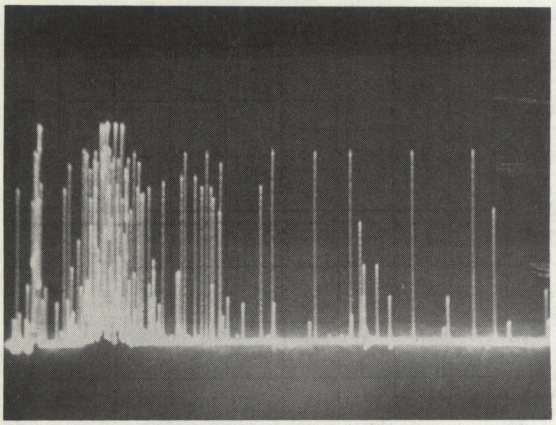

Figure 5. Typical UV return signal. Abscissa is height (one division = 3 km range) and ordinate is signal strength. Spikes correspond to detection of single UV photons. Region of full beam overlap begins at about 9 km msl.

particular broad-band glass UV filter was not optimum for the experiment, yet the background noise was negligible at Mauna Loa from late twilight through the night. Measurements of background during the day indicate that daytime operation will be possible with a narrow band filter and a smaller field of view for the receiver.

Figure 7 shows a return with the UV filter removed from the receiver. We now get the return from the yellow fundamental of the laser at about 590 nm. The flat-topping is due to saturation of the transient digitizer. The figure shows a strong atmospheric return from heights well past 30 km msl. This return is useful for estimating Mie scattering layers to be used in the ozone analysis, as explained in a previous section.

We did not attempt to analyze the measurements of the UV signal for ozone vertical distribution because poor doubled-laser performance precluded alignment optimization and prevented accumulation of sufficient detected photons per range element to yield a statistically meaningful result.

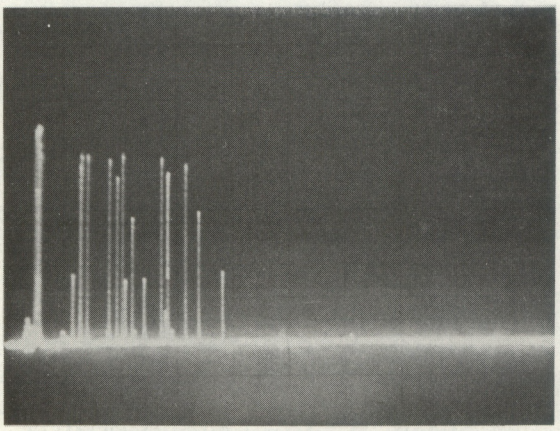

Figure 6. UV return for very small transmitted energy. Note the absence of background or leakage photons above 15 km, the maximum range of the transmitted UV signal.

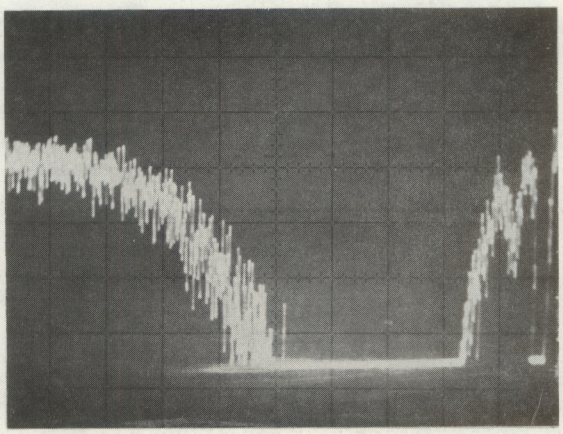

Figure 7. Return signal with UV filter removed from receiver. Note strong signal from 30 km and above. Flat top is due to electronic saturation.

7. LASER PERFORMANCE

The primary reason for the failure to obtain ozone density profiles was a two-order magnitude shortfall in UV output energy available from the laser. Subsequent investigation of the laser performance at the GE Corporate Research and Development Laboratories revealed that the failure to achieve good, reliable doubling efficiency was due to the fluctuations in the spectral distribution of the dye laser output. We were unable to optimize the laser prior to the experiment because of late delivery.

In a 1976 demonstration of frequency doubling at the Phase-R Labs, it was relatively easy to achieve 10% power conversion. That is, an input pulse with a peak power of 1 MW could be doubled reliably to produce a peak output of 0.1 MW. However, the time duration of the output pulse was much shorter than that of the input, so the energy conversion, as opposed to the power conversion, was much less than 10%. Under optimum laboratory conditions, it was possible to produce 10% energy conversion at times, but the reliability was poor. To make reliable ozone profile measurements, the laser system would have had to be refined so that reliable operation could be attained under field conditions.

In the same year, the reliability of the Chromatix Corp. laser system was excellent, but the UV pulse energy was only about 1 mJ. However, the firing rate was more than 10 pulses per second, so adequate transmitted energy could be attained in reasonable times.

Within the last two years, the capability of UV lasers has increased substantially. For example, a proven Quanta-Ray Nd:YAG laser system provides 200 mJ per pulse at the doubled wavelength of 532 nm at 10 pulses per second. It has been well demonstrated that this laser can pump a dye laser at 50 mJ per pulse, doubling to 10 mJ per pulse at about 300 nm, providing 100 mW power at the UV wavelength. Another example is a flashlamp-pumped Candela dye laser, which can provide at least 0.4 J per pulse at 10 pulses per second in the blue (450-490 nm) or red (540-620 nm). The red beam can be doubled with 5% to 10% efficiency to provide at least 200 mW average power at appropriate wavelengths around 300 nm.

These laser systems cost between $20,000 and $30,000. Each provides exceptional capabilities for ozone measurements. For example, from Fig. 3 it is evident that ozone density to altitudes well above the ozone maximum can be measured on a time scale commensurate with changes in the level.

8. MEASUREMENT POTENTIAL

Initial ultraviolet DIAL experiments in 1975, one of which is described here, provided experience with techniques that can now yield detailed measurements of the distribution of upper tropospheric and stratospheric ozone up to and somewhat beyond the ozone maximum (between 20 and 30 km msl). In addition to the reports by Megie et al. (1977) of their successful results in the UV, fourteen papers presented at the 8th International Laser Radar Conference, held at Drexel University from June 6 to June 9, 1977, concerned DIAL measurements of O_3, NO_2, H_2O, SO_2, and other species.

A recent article by Remsberg and Gordley (1978) considers similar measurements of ozone from a space shuttle platform.

All of the experiments reported thus far have been "proof-of-principle" experiments. Taken together, the experimental and analytical work has established an excellent technical formation for establishment of a facility to provide extensive monitoring observations. The most valuable initial application for such a facility might well be a study of circulation and ozone diffusion in the upper troposphere and lower stratosphere. Such studies should reveal much new information about the dynamics of circulation and diffusion near the tropopause. This information would be particularly interesting now because of the anticipated effects of long-lived gases introduced into the troposphere, such as chlorine-bearing molecules and N_2O, on stratospheric ozone.

9. CONCLUSIONS

Ultraviolet differential absorption lidar (DIAL) returns were observed at the Mauna Loa facility. Although these returns were too weak to allow interpretation in terms of ozone density, valuable experience was gained. Subsequent successful measurements by Megie et al., among others, have demonstrated the viability of the technique. In particular, ground-based UV DIAL now offers practical remote measurements of ozone and general gas circulation at or near the tropopause and on up to well beyond the ozone maximum.

10. ACKNOWLEDGMENTS

We gratefully acknowledge the untiring assistance of Howard T. Ellis of the NOAA Mauna Loa Observatory, who provided essential assistance in the setup and data-taking of the experiment, often under adverse conditions. We also appreciate the help given by W. Komhyr and S. Oltmans in logistical support from the NOAA Labs in Boulder.

Thanks are also due to Drs. Lester Machta and Kirby Hanson of the NOAA Air Resources Lab and to the General Electric Corporate Research and Development Laboratories for making funds and equipment available to perform this work.

11. REFERENCES

1. Air Force Geophysical Research Office, 1960: Ozone cross sections, ch. 16, In: Handbook of Geophysics. Macmillan, pp. 16.21-16.25.

2. Climatic Impact Assessment Program, 1975: The natural stratosphere of 1974. CIAP Monogr. 1, DOT-TST-75-51, Nat. Tech. Inf. Serv., Springfield, Virginia.

3. Global Atmospheric Research Program, 1975: The physical basis of climate and climate modelling. GARP Publ. Ser. No. 16, World Meteorol. Org., p. 66.

4. Gibson, A. J., and L. Thomas, 1975: Ultraviolet laser sounding of the troposphere and lower stratosphere. Nature, 256:561-563.

5. Geophysical Monitoring for Climatic Change, 1977: Geophysical monitoring for climatic change, No. 5, Summary report, 1976. K. Hanson, ed. NOAA ERL.

6. Hering, W. S., and T. R. Borden, Jr., 1965: Mean distributions of ozone density over North America, 1963-1964. AFCRL-65-913.

7. McCormick, M. P., 1977: The use of lidar for stratospheric measurements. Invited paper at 8th International Laser Radar Conference, June 6-9, 1977, Drexel University, Philadelphia, Pennsylvania.

8. Megie, G., J. Y. Allain, M. L. Chanin, and J. E. Blamont, 1977: Vertical profile of stratospheric ozone by lidar sounding from the ground. Nature, 270:329-331.

9. Penney, C. M., 1974: Resonance Raman scattering from ozone. Paper presented at the 1974 International Laser Radar Conf., Sendai, Japan, Sept. 1974.

10. Penney, C. M., 1975: Remote measurement of ozone by resonant Raman scattering and differential absorption. Proc. Conf. Laser Eng. and Appl., May 28-30, 1975, Washington, D. C.

11. Remsberg, E. E., and L. L. Gordley, 1978: Analysis of differental lidar from the space shuttle. Applied Optics, 17:624-630.